Numerical Study on the Performance of NACA 4412 Airfoil with Insertion of Tangential Internal Slot

Sk Samiul Basir, Md. Imtiaze Bulbul, Mohammad Ali*

Department of Mechanical Engineering, Bangladesh University of Engineering and Technology, Dhaka-1000, Bangladesh

**Email address for correspondence: mali@me.buet.ac.bd*

Keywords: NACA 4412, passive control, internal slot, tapered slot, lift-to-drag ratio

Abstract

Controlling flow separation is one of the most important techniques for reducing drag and increasing the lift-to-drag ratio. The aim of this study is to enhance the aerodynamic performance of NACA 4412 airfoil through passive method of controlling flow separation. Accordingly, as a method of passive control, the geometry of airfoil has been modified with tangential internal slots. The commencement of each slot is kept constant at 0.05 chord(C) from the leading edge. The exit positions of the slots are varied vertically at 0.4C slot exit. So, two parameters have been varied: slot width and vertical slot exit position. The angles of attack (AoA) are varied from 0^0 to 26^0 with 2^0 increments for every parameter with a fixed Reynolds number of 1.6×10^6. Pressure-based solver and k-ω SST model are used for analysis. For all the slot configurations, better aerodynamic performance in terms of lift-to-drag ratio occurs at the moderately higher angles of attack. Among the vertical exit position, the lowermost position shows better aerodynamic performance. Tapered slot having slot exit width 2%C has higher lift-to-drag ratio than that of the other configurations from AoA 6^0 to the end. However, the highest lift-to-drag ratio is found at AoA 8^0 for all the modified designs whereas it happens at AoA 6^0 for the airfoil with no slot. Moreover, for this configuration, the stalling angle of attack is delayed to AoA 24^0 whereas for other configurations the stall angle gradually decreases and for no slot it is the lowest which is AoA 16^0.

1 Introduction

Flow separation is a phenomenon that affects adversely the aerodynamic performance, especially at higher angles of attack. By modifying the wing shape, flow separation can be delayed.

In many research papers, active and passive control mechanisms are studied. As an active method suction, blowing etc. can be introduced. As a passive method internal slot, vortex generator etc. can be introduced. Yousefi et al. [1] looked at how a NACA 0012 airfoil's blowing and suction flows were affected by jet width. As an active method, Azim et al. [2] had shown the delay of flow separation of 2D NACA 4412 airfoil by suction.

Moshfeghi et al. [3] investigated the aerodynamic performance of a horizontal axis wind turbine by splitting the blades along the span. Belamadi et al. [4] studied the aerodynamic performance of slotted airfoils and found that the modified airfoil performs better at higher angles of attack than solid airfoil.

The aerodynamic performances were improved for a range of angle of attack. Ni et al. [5] investigated how the internal slot and crosswise leading-edge tubercles of an airfoil affect its performance as a whole. It was shown that the slot made a big difference in the performance after the stall angle.

Saman Beyahaghi et al. [6] found an increment in the lift coefficient while the drag coefficient remained approximately unchanged by investigating a slotted airfoil. Younghui Xie et al. [7] investigated the control of flow separation for S809 airfoil with slots both numerically and experimentally. The results showed improvement of the blade aerodynamic efficiency. Fawzi et al. [8] studied straight-slotted NACA 4412 airfoil and showed that the slotted airfoil outperforms the baseline configuration along with a delayed stalling angle. Flow separation is more affected by slots at higher angles of attack and hence overall aerodynamic performance is improved. Akshoy et al. [9] investigated flow separation control over a NACA 2412 airfoil with slot and found that the slotted airfoil shows better aerodynamic performance compared to the airfoil without slot, particularly at higher angles of attack.

The present study is performed to investigate the performance of airfoil through the insertion of tangential internal slots. The slot's entry and exit positions along the chord are kept fixed. The vertical locations of slot exits are varied. Next, the effects of vertical exit locations are compared. Slot widths are varied to evaluate the impact of slot width. Lastly, tapered slots are introduced and their effect on aerodynamic performance is studied.

2 Methodology

2.1 Governing Equations

The governing equations of fluid dynamics are Navier-Stokes equations. These equations can be expressed as follows:

Continuity equation: $\frac{\partial u}{\partial x} + \frac{\partial v}{\partial y} + \frac{\partial w}{\partial z} = 0$ (1)

$$x\ momentum:\ \rho(\frac{\partial u}{\partial t} + u\frac{\partial u}{\partial x} + v\frac{\partial u}{\partial y} + w\frac{\partial u}{\partial z}) = -\frac{\partial p}{\partial x} + \rho f_x + \mu(\frac{\partial^2 u}{\partial x^2} + \frac{\partial^2 u}{\partial y^2} + \frac{\partial^2 u}{\partial z^2}) \quad (2)$$

$$y\ momentum:\ \rho(\frac{\partial v}{\partial t} + u\frac{\partial v}{\partial x} + v\frac{\partial v}{\partial y} + w\frac{\partial v}{\partial z}) = -\frac{\partial p}{\partial y} + \rho f_y + \mu(\frac{\partial^2 v}{\partial x^2} + \frac{\partial^2 v}{\partial y^2} + \frac{\partial^2 v}{\partial z^2}) \quad (3)$$

$$z\ momentum:\ \rho(\frac{\partial w}{\partial t} + u\frac{\partial w}{\partial x} + v\frac{\partial w}{\partial y} + w\frac{\partial w}{\partial z}) = -\frac{\partial p}{\partial z} + \rho f_z + \mu(\frac{\partial^2 w}{\partial x^2} + \frac{\partial^2 w}{\partial y^2} + \frac{\partial^2 w}{\partial z^2}) \quad (4)$$

For turbulent formulation, the RANS equation is used for incorporating turbulent viscosity.

The standard SST κ-ω turbulence model is used to simulate the turbulent flow around the configurations.

The turbulence kinetic energy, k, and the specific dissipation rate, ω, are obtained from the following transport equations:

$$\frac{\partial}{\partial t}(\rho k) + \frac{\partial}{\partial x_i}(\rho k u_i) = \frac{\partial}{\partial x_j}(\Gamma_k \frac{\partial k}{\partial x_j}) + G_k - Y_k + S_k + G_b \quad (5)$$

And

$$\frac{\partial}{\partial t}(\rho\omega) + \frac{\partial}{\partial x_i}(\rho\omega u_i) = \frac{\partial}{\partial x_j}(\Gamma_\omega \frac{\partial \omega}{\partial x_j}) + G_\omega - Y_\omega + D_\omega + S_\omega + G_{wb} \quad (6)$$

In these equations, $G_k$is the generation of turbulent kinetic energy. G_ω is the generation of specific dissipation rate ω. Γ_k and Γ_ω are the effective diffusivity of κ and ω, respectively. Y_k and Y_ω indicate the dissipation of κ and ω due to turbulence. S_k and S_ω represent terms of user defined source . Buoyancy terms are expressed by G_b and G_{wb} .

2.2 Geometry

NACA 4412 airfoil of chord length 1 m is selected for this study. Figure *1* shows the geometry of the NACA 4412 airfoil.

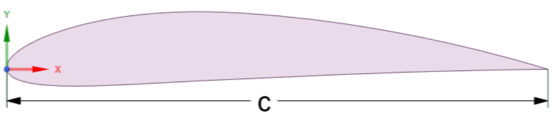

Figure 1: Baseline airfoil

The commencement of each slot is kept constant at Y=5%C chord length from the leading edge. *Figure 2* shows the shape of a generic internal slot of uniform width where the circular arc is ended tangentially at x=40%C of the suction surface. There the suction surface is cut by a vertical cutting plane with a length of Z= 2.5%C and the rest of the portion to the trailing edge is cut tangentially. Then the slot exit positions are varied along that vertical line.

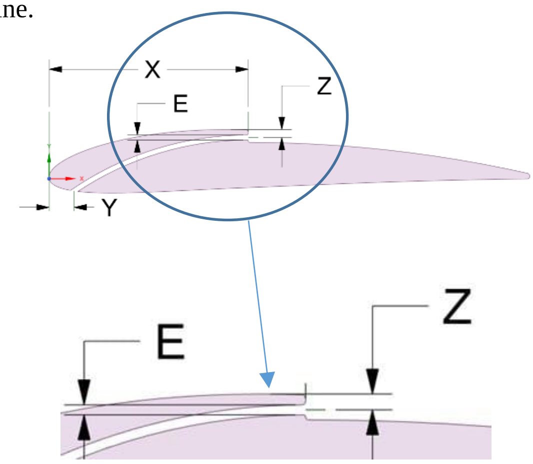

Figure 2: Airfoil geometry for present study with uniform slot

Designs considered for uniform slot width with slot entry at Y=5%C and exit at X= 40%C are given in *Table 1*.

Table 1: Parameter of Uniform Width Slot Design at slot exit X= 40%C

Design	'E'	'Z'
A1	1%C	1%C
A2	1%C	1.5%C
A3	1%C	2%C
A4	1.5%C	1.75%C
A5	2%C	1.5%C

Here 'X' is the horizontal distance from the leading edge to the slot exit along the chord line. 'Y' is the horizontal distance from the leading edge to the center of uniform slot entrance position. 'B' is the horizontal length of slot width at entrance. 'E' is the slot exit width. 'Z' is the vertical distance from the top surface of airfoil to the center of slot exit.

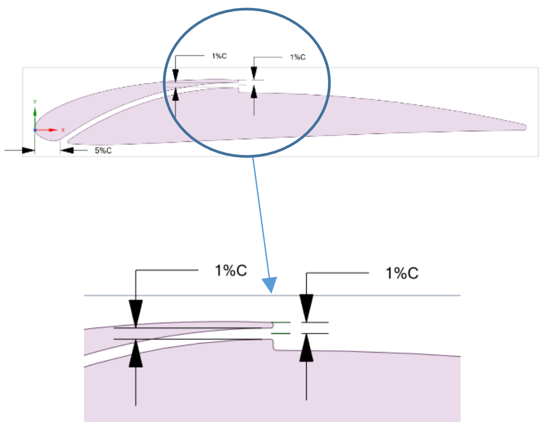

(a)

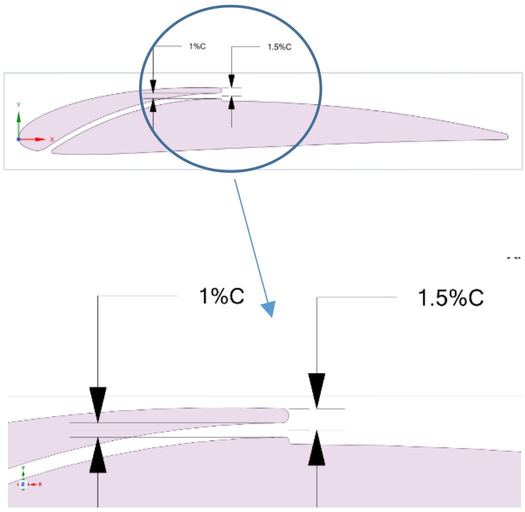

(b)

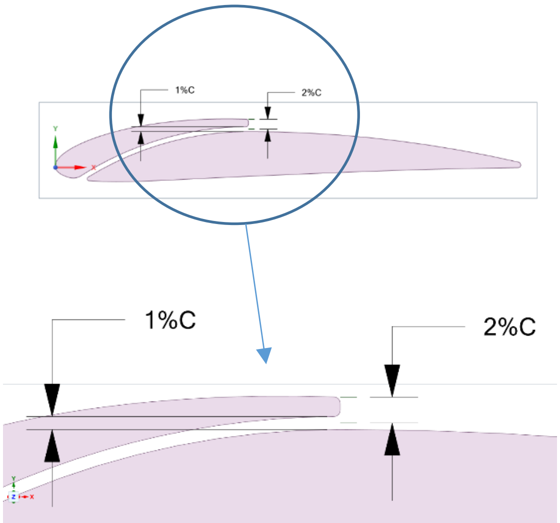

(c)

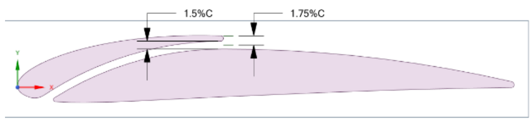

(d)

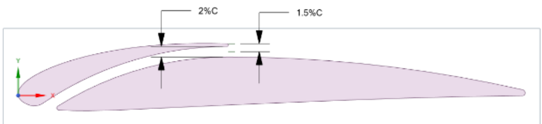

(e)

Figure 3: Design (a) A1, (b) A2, (c) A3, (d) A4, (e) A5

Additionally, three tapered slot configurations are considered for each exit position. *Figure 3* shows all the shape of internal slots of uniform width. The slots exits width are kept 1%C, 1.5%C and 2%C. Figure *4* shows the generic configuration for all the considered tapered slots.

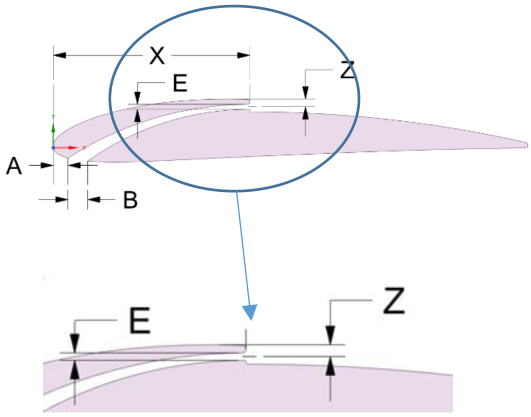

Figure 4: Airfoil geometry for present study with tapered slot

Designs considered for tapered slot width with slot exit at 40%C are given in *Table 2*

Table 2: Parameter of Uniform Width Slot Design at slot exit X= 40%C.

Design	A	B	E	Z
B1	3%C	4%C	1%C	2.5%C
B2	2%C	6%C	1.5%C	1.75%C
B3	1%C	8%C	2%C	1.5%C

Here 'X' is the horizontal distance from the leading edge to the slot exit along the chord line. 'A' is the horizontal distance from the leading edge to the slot entrance starting position. 'B' is the horizontal length of slot width at entrance. 'E' is the slot exit width. 'Z' is the vertical distance from the top surface of airfoil to the center of slot exit.

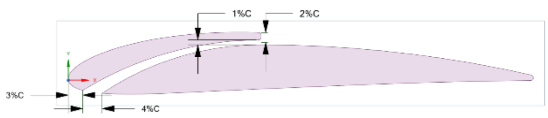

(a)

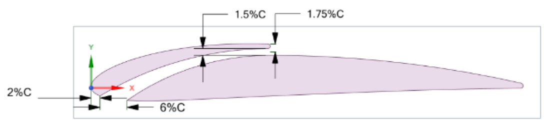

(b)

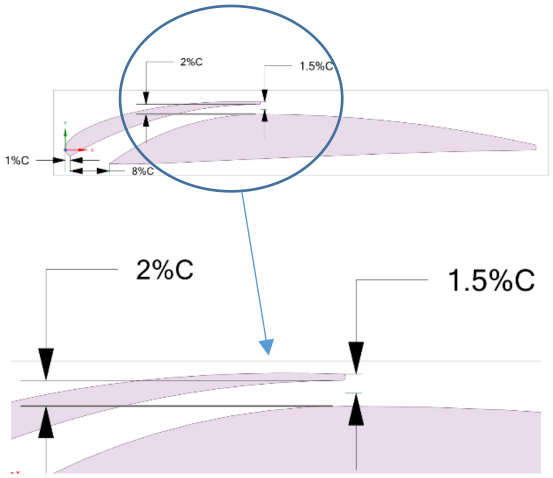

(c)

Figure 5: Design (a) B1, (b) B2, (c) B3

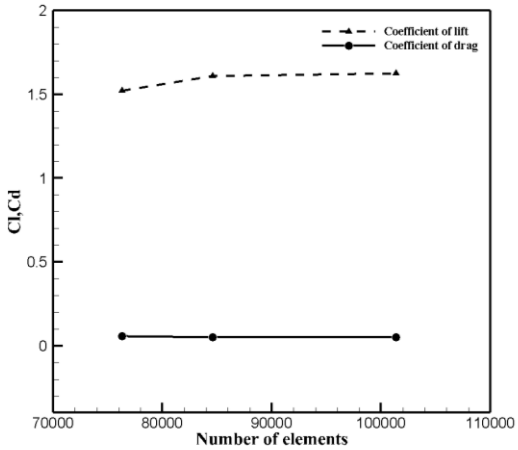

Figure 7: Mesh independency test

2.3 Numerical Solution

The geometric model is developed initially by "ANSYS SPACECLAIM" for mathematical modelling. "ANSYS FLUENT" is used for numerical solutions, which works based on the finite volume technique. To simulate the flow around the airfoil arrangement, C-domain is used.

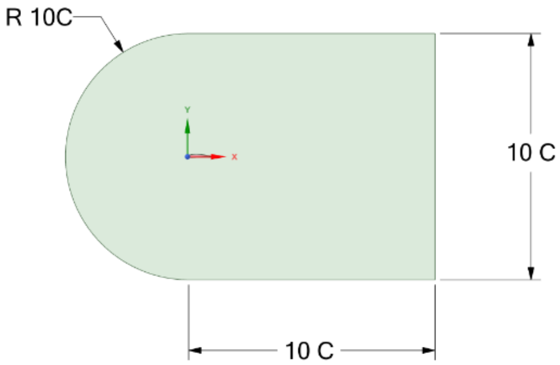

Figure 6: Computational domain

2.4 Grid Generation

Hybrid meshing with polyhedral elements is done in FLUENT MESHING. The chord and span length of the airfoil are set to 1 m and 0.1 m. Computations are performed for mesh independency test for 3 different mesh. They are composed of 76290, 84269, and 101374 elements. Element of 76290 is selected as this

Figure 7 shows the lift coefficient and drag coefficient at AoA 16^0 for different mesh sizes. For all of them, element density is kept high around the surface of the airfoil to capture the boundary effect properly. 20 inflation layer is taken around the airfoil surface for the wall y+ requirement corresponding to κ-ω SST turbulence model.

3 Results and discussion

3.1 Validation

At first, validation is required for ensuring the reliability of the simulation. The validation process is done by comparing the current data of no slot NACA 4412 airfoil with 2D Numerical data by Fawzi et al. [8] for Re = 1.6×10^6.

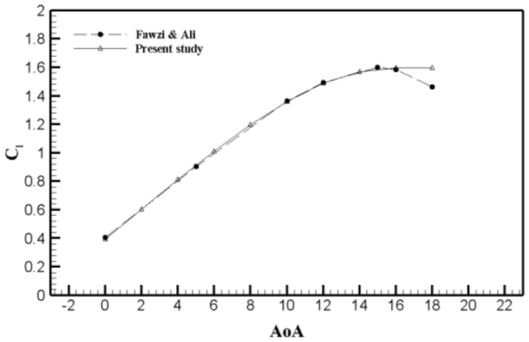

Figure 8: Comparison of lift coefficient

Figure 8 and Figure 9 show that the current study aligns almost close to the numerical data of Fawzi et al [8]. From Figure 9, the maximum *variation* of lift coefficient from the literature is for AoA 18^0. We have taken 3D geometry in our simulation and Fawzi et al [8] have taken 2D geometry in their study. This might one of the reasons behind the variations from literature.

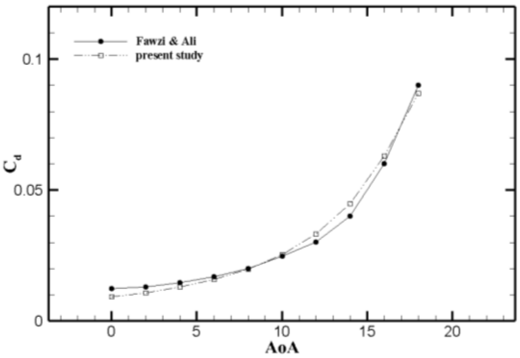

Figure 9: Comparison of drag coefficient

3.2 Effects of the internal slot on aerodynamic performance

To evaluate the aerodynamic performance, the coefficient of drag, coefficient of lift and lift-to-drag ratio of the slotted airfoil are compared with those of solid airfoil. For all the taken designs, drag coefficients are compared in *Figure 10*. At the higher angles of attack, the drag coefficient of the slotted airfoil decreases than no slot airfoil. Because flow separation was delayed due to the slots. Design B3 shows better improvement to drag performance among all the designs. For design B3, drag performance improves from AoA 5^0. The maximum improvement of the drag coefficient is 48.86% at AoA 20^0.

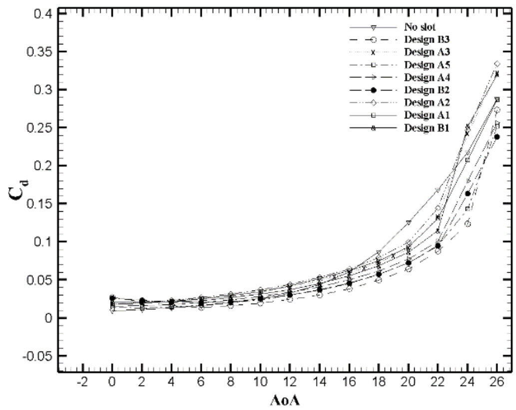

Figure 10: Variation of drag coefficient with angle of attack

From Figure 11 it is evident that at a higher angle of attack lift performance also starts improving. Among all the slot configurations, design B3 shows maximum improvement. For design B3 the lift characteristic begins to be superior after AoA 12^0. For design 0.4C B3, lift performance improves from AoA 12^0. Stalled angle has occurred at AoA 24^0. The maximum improvement of lift coefficient is 54.94% at AoA 24^0.

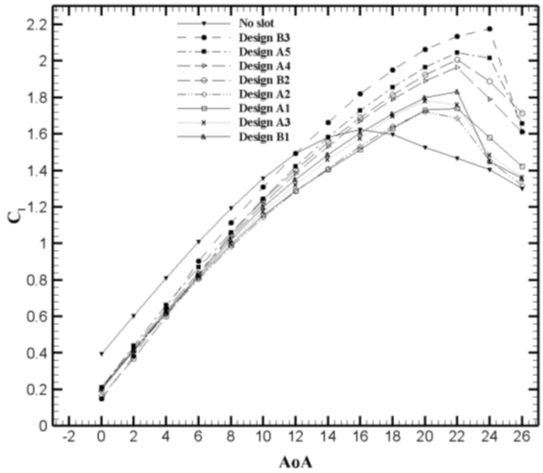

Figure 11: Variation of lift coefficient with angle of attack

Figure 12 shows the overall lift-to-drag ratio comparison among all the slotted airfoils with no slot airfoil. Among the uniform width 1%C slot design A1, A2 and A3, a better lift-to-drag ratio is obtained for A3. Then the slot width is increased to 1.5%C and 2%C for designs A4 and A5 at the same exit location as A3. This time A5 performs better than the others. At last, tapered slot designs B1, B2 and B3 are considered at the same exit point of design A3. The aerodynamic performance was improving with increasing the tapered width. A ratio of 4 is maintained for slot entry and exit width of the tapered slot. Design B3 shows superior performance than the other design at higher angles of attack. So, design B3 is the optimized design.

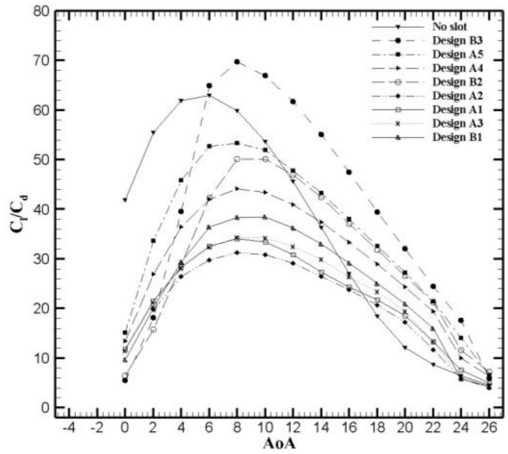

Figure 12: Variation of lift-to-drag ratio with the angle of attack

For Design B3, the lift-to-drag ratio improves After AoA 6^0. So the effective range for design is AoA 6^0 to AoA 24^0. The maximum lift-to-drag ratio is found at AoA 8^0 for design B3. At AOA 14^0 lift-to-drag ratio improvement is 51.63%. At AOA 16^0 lift-to-drag ratio improvement is 75.69%. At AOA 18^0 lift-to-drag ratio improvement is 114.39%. At AOA 20^0 lift-to-drag ratio improvement is 164.34%. The maximum amount of lift-to-drag ratio improvement is 179.75% at AoA 22^0. At AoA 24^0 lift-to-drag ratio improvement is 172.85%.

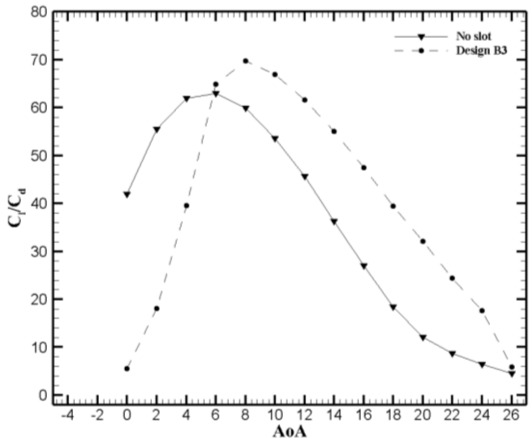

Figure 13: Variation of lift-to-drag ratio with the angle of attack for optimized design and no slot airfoil

Figure 14 shows the velocity contour at AoA 20^0 for no slot and slotted design B3. The figure shows the effect of the slot on flow separation. Flow separation is delayed to the trailing edge of the slotted airfoil.

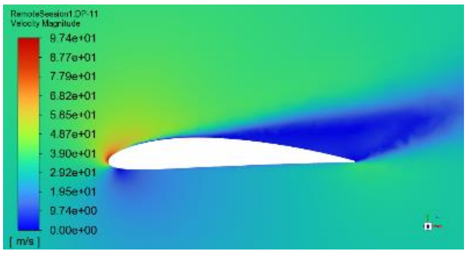

(a)

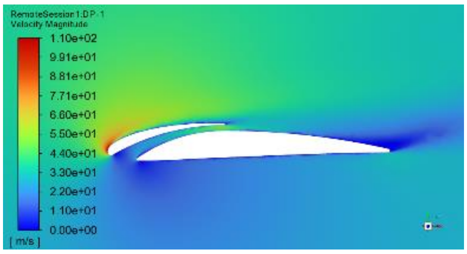

(b)

Figure 14: Velocity contour at AoA 20 for (a) No slot airfoil (b) Design B3

Figure 14 shows the velocity contour at the angle of attack 24^0 for no slot and slotted B3 design. The figure also shows the delay of flow separation clearly.

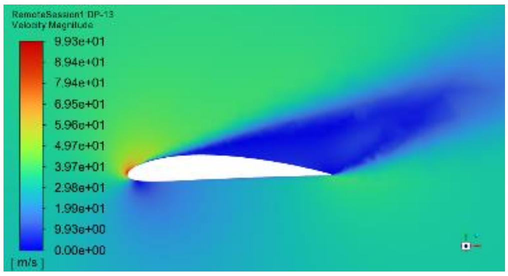

(a)

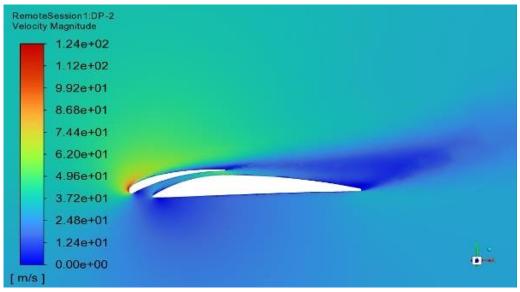

(b)

Figure 15:Velocity contour at AoA 24^0 for (a) solid NACA 4412 (b) Design B3

For no slot airfoil flow separation has occurred at 0.3C. Flow separation is delayed to 0.85C at AoA 24^0 for design B3.

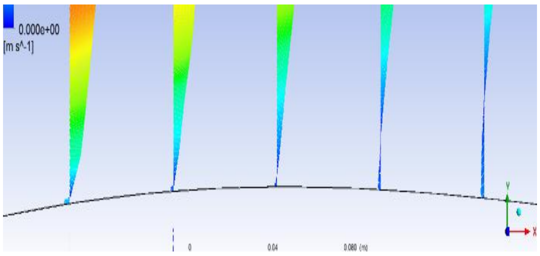

(a)

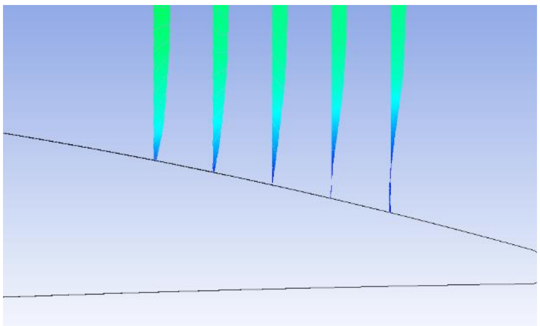

(b)

Figure 16: Flow separation at AoA 24^0 (a) No slot airfoil, (b) Design B3

4 Conclusion

A parametric study has been done considering slot width and vertical location of slot exit and the results are compared with no slot in NACA 4412 airfoil.

For no slot airfoil, at higher angles of attack flow separation becomes dominant which leads to make more adverse pressure gradient and stalling occurs at AoA 16^0. All slot configurations show superior lift to drag ratio in angles of attack more than 18^0. Additionally, a slotted airfoil with lower angles of attack exhibits a detrimental impact. Among all the uniform slot exit vertical locations, aerodynamic performance is better for the lowermost slot exit. When slot width is increased from 1%C to 1.5%C and 2%C, better aerodynamic performance is found for increased slot width. Performance of all considered tapered width slots are better than corresponding uniform width slots. Optimized slot is the design B3 (tapered slot exiting with 2%C width). For the optimum slot configuration, the lift characteristic begins to be superior after AoA 12^0 and stalling occurs at AoA 24^0. The drag coefficient decreases after AoA 5^0 for the optimized slot and for the other cases decreases later compared to no slot airfoil. The difference of lift-to-drag ratio between the optimized slot and no slot airfoil is remained negative up to AoA 6^0 and become positive up to 26^0. However, maximum difference of lift-to-drag ratio between the optimized design and no slot airfoil is found at AoA 18^0.

5 References

[1] Yousefi,K.,Saleh,R., and Zahedi, P., ‘Numerical study of blowing and suction slot geometry optimization on NACA 0012 airfoil’, Journal of Mechanical Science and Technology, Vol 28 (4), pp. 1297-1310,2014.

[2] Azim,R., Hasan, M.M., and Ali,M., ‘Numerical Investigation on the Delay of Boundary Layer Separation by Suction for NACA 4412’, 6th BSME International Conference on Thermal Engineering (ICTE 2014), Procedia Engineering, Vol 105, pp.329-334,2015.

[3]Moshfeghi, M.,Shams,S.,and Hur, N., ‘Aerodynamic performance enhancement analysis of horizontal axis wind turbines using a pasive flow control method via split blade’,Journal of Wind Engineering and Industrial Aerodynamics, Vol 167, pp. 148-159,2017.

[4] Belamadi,R.,Djemili,A., Ilinca, A., and Mdouki, R., ‘Aerodynamic performance analysis of slotted airfoils for application to wind turbine blades’, Journal of Wind Engineering and Industrial Aerodynamics, Vol 151, pp.79-99,2016.

[5] Ni,Z., Dhanak, M., and Su,T., ‘Performance Characteristics of Airfoils with Leading-Edge Tubercles and an Internal Slot’, AIAA Journal, Vol 57 (1),pp. 1-14, 2019.

[6] Beyhaghi, S., S. Amano, R., ‘ A parametric study on leading-edge slots used on wind turbine airfoils at various angles of attack’, Journal of Wind Engineering and Industrial Aerodynamics, Vol. 175, Pp. 43–52, 2018

[7] Xie, Y., Chen, J., Qu, H., Xie, G., Zhang, D., and Moshfeghi, M., ‘Numerical and experimental investigation on the flow separation control of S809 airfoil with slot’, Mathematical Problems in Engineering, 2013.

[8] Fawzi, S., Hamid Ali, A., ‘Slot Design Procedure for a NACA 4412 at High Angle of Attack’, Journal of Mechanical Engineering Research and Developments, vol 44(8), pp. 188-203, 2021

[9] Paul, A.R., Mittal, A., Jain, A,. ‘Slotted Flow Separation Control Over A Naca 2412 Airfoil’, Proceedings of 39th National Conference on Fluid Mechanics & Fluid Power (FMFP-2012),, At NIT, Surat, Gujarat,, Vol. Paper Code, 39.